Final parsec problem of black hole mergers and ultralight dark matter

Hyeonmo Koo[a†], Dongsu Bak[a,b†], Inkyu Park[a,b], Sungwook E. Hong[c,d] , Jae-Weon Lee[e*]
a) Physics Department, University of Seoul, Seoul 02504, Korea
b)Natural Science Research Institute, University of Seoul, Seoul 02504, Korea
c) Korea Astronomy and Space Science Institute, 776 Daedeok-daero, Yuseong-gu, Daejeon 34055, Korea
d) Astronomy Campus, University of Science and Technology, 776 Daedeok-daero, Yuseong-gu, Daejeon 34055, Korea
e) Department of Electrical and Electronic Engineering, Jungwon University, 85 Munmuro, Goesan, Chungbuk 28024, Korea

(Dated: November 8, 2023)

When two galaxies merge, they often produce a supermassive black hole binary (SMBHB) at their center. Numerical simulations with cold dark matter show that SMBHBs typically stall out at a distance of a few parsecs apart, and take billions of years to coalesce. This is known as the final parsec problem. We suggest that ultralight dark matter (ULDM) halos around SMBHBs can generate dark matter waves due to gravitational cooling. These waves can effectively carry away orbital energy from the black holes, rapidly driving them together. To test this hypothesis, we performed numerical simulations of black hole binaries inside ULDM halos. Our results imply that ULDM waves can lead to the rapid orbital decay of black hole binaries.

arXiv:2311.03412v1 [astro-ph.GA] 6 Nov 2023

I. INTRODUCTION

The mystery of supermassive black hole (SMBH) growth is one of the unsolved problems in astronomy. When two galaxies merge, they can form a supermassive black hole binary (SMBHB) at their center. However, numerical simulations show that SMBHBs typically become stuck at a distance of a few parsecs apart, and can take billions of years to merge. At this distance the density of the stars and gas near the SMBHB is too low for dynamical friction to be efficient, while the loss of orbital energy of the SMBHB due to gravitational waves is only efficient for distances less than $\mathcal{O}(10^{-2})$ pc [1, 2]. Furthermore, the loss cone is depleted as the black holes (BHs) approach each other. This difficulty is known as the final parsec problem. The gravitational wave background recently observed by NANOGrav [3] is usually attributed to efficient SMBH mergers. This fact deepens the mystery. Proposed solutions to the final parsec problem often involve bringing in extra matter, such as additional stars or another BH interacting with the black hole binaries (BHBs) to help them merge.

Ultralight (fuzzy) dark matter (ULDM) [4–9] is a promising alternative to cold dark matter (CDM), as it has the potential to solve some of the small-scale issues of CDM such as the missing satellites problem, the plane of satellite galaxies problem and the core-cusp problem [10–13]. In this model, the ULDM is in a Bose-Einstein condensate (BEC) state of ultralight scalar particles with a typical mass $m \gtrsim 10^{-22}\,\mathrm{eV}/c^2$. ULDM can be described with a macroscopic wave function ψ and the uncertainty principle suppresses too many small-scale structure formations. Beyond the galactic scale, the ULDM behaves like CDM, and hence naturally solves the problems of CDM. This model has been also shown to be able to explain a wide range of astrophysical observations, including the rotation curves of galaxies [8, 14, 15], and the large-scale structures of the universe [16]. Recently, there has been a growing interest in the interactions between BHs and ULDM halos surrounding them [17], as these interactions could change the patterns of gravitational waves generated by BHBs.

In this letter, we suggest that, inside ULDM halos (for a review, see [18–23]), BHBs can generate dark matter (DM) waves due to gravitational cooling [24], which is a mechanism for relaxation by ejecting ULDM waves carrying out excessive kinetic energy and momentum. These waves can effectively carry away orbital energy from the BHB, rapidly driving them together and possibly solving the final parsec problem. To test this hypothesis, we perform numerical simulations of BHBs at $\mathcal{O}$(pc) separation in a ULDM soliton representing a core of the galactic halos. Our results provide some evidence that DM waves could lead to the rapid orbital decay of the BHs.

The aim of this paper is to numerically show orbital decays of BHBs due to gravitational cooling of ULDM, whose dynamics is described by the Schrödinger-Poisson equations. The structure of this paper is organized as follows. In Sec. II, we explain our numerical simulation for studying the orbital decay of BHBs. Then, Sec. III and IV show the numerical results from Sec. II and their theoretical analyses, respectively. Finally, Sec. V summarizes our work.

*Electronic address: dsbak@uos.ac.kr,icpark@uos.ac.kr, swhong@kasi.re.kr, scikid@jwu.ac.kr; † These authors contributed equally to this work.

II. SIMULATION

In our simulation, we shall treat BHs as point particles with the Newtonian gravity. The post-Newtonian correction to the gravitational potential of a BH at a distance of r from the BH is on the order of r_s/r, where $r_s = 2GM_{\rm bh}/c^2$ is the Schwarzschild radius of the black hole. For $M_{\rm bh} = 10^8 {\rm M}_\odot$ and $r = 0.01\,{\rm pc}$, this correction is $\mathcal{O}(10^{-3})$. Therefore, the Newtonian approximation of the gravitational field is good enough for our calculation.

The ULDM system, interacting gravitationally with N-particles (BHs), is governed by the Schrödinger-Poisson equations

$$i\hbar\frac{\partial}{\partial t}\psi(\mathbf{x},t) = -\frac{\hbar^2}{2m}\nabla^2\psi(\mathbf{x},t) + m\left[V_{\rm U}(\mathbf{x},t) + V_{\rm N}(\mathbf{x},t)\right]\psi(\mathbf{x},t) \tag{1}$$

$$\nabla^2 V_{\rm U}(\mathbf{x},t) = 4\pi G\,|\psi|^2(\mathbf{x},t) \tag{2}$$

with the mass m of ultralight DM particles and the Newton constant G. The wave function $\psi(\mathbf{x},t)$ for ULDM is a complex function of spacetime normalized as $\int d^3\mathbf{x}\,|\psi|^2 = M$ with M denoting the total ULDM mass such that the corresponding ULDM mass density is given by $\rho = |\psi|^2$. $V_{\rm U}$ is the potential from the ULDM mass distribution and $V_{\rm N}$ for the N-particles where k-th ($k = 1, 2, \cdots, N$) particle is located at $\mathbf{x}_k(t)$ with mass M_k. (In this work, $N = 2$.) Then, the N-body potential is given by $V_{\rm N}(\mathbf{x},t) = \sum_{k=1}^{N} V_k(\mathbf{x},t)$ with $V_k(\mathbf{x},t) = -GM_k/|\mathbf{x} - \mathbf{x}_k(t)|$. With these potentials, the remaining N-body dynamics is described by

$$\ddot{\mathbf{x}}_k(t) = -\nabla V_{\rm U}(\mathbf{x}_k(t),t) - \sum_{l\neq k}\nabla V_l(\mathbf{x}_k(t),t)\,. \tag{3}$$

The total combined system enjoys two exact scaling relations. One is related to the scaling of the total ULDM mass M and the particle mass M_k: $[\,M,\ M_k,\ m,\ t,\ \mathbf{x},\ V_{\rm U},\ V_k,\ \psi\,] \to [\,\kappa M,\ \kappa M_k,\ m,\ \kappa^{-2}t,\ \kappa^{-1}\mathbf{x},\ \kappa^2 V_{\rm U},\ \kappa^2 V_k,\ \kappa^2\psi\,]$. The other is the scaling of the ULDM particle mass m with the transformation $[\,M,\ M_k,\ m,\ t,\ \mathbf{x},\ V_{\rm U},\ V_k,\ \psi\,] \to [\,M,\ M_k,\ \lambda m,\ \lambda^{-3}t,\ \lambda^{-2}\mathbf{x},\ \lambda^2 V_{\rm U},\ \lambda^2 V_k,\ \lambda^3\psi]$. Under these two transformations, the forms of the full equations (1), (2) and (3) remain invariant. These two scaling relations will be useful in the theoretical analysis in Sec. IV.

In our simulation, we use the Python pseudo-spectral solver, PyUltraLight2 [25], which is publicly available. This package, as in its prior version [26], solves the Schrödinger-Poisson equations but also incorporates the above-mentioned N-body dynamics in a full-fledged form. In this package, the system will be placed in a box of size L with a periodic boundary condition $x_i \sim x_i + L$. Below we take the box size to be $L = 40\,{\rm pc}$, which is large enough to neglect the effect of the periodic boundary condition. The number of grid size in each direction is taken to be 500, and then the resulting spatial resolution becomes $\Delta x = 0.08\,{\rm pc}$.

We choose our time resolution to be $\Delta t = 1.042\,m_{21}^{-1}\,{\rm yr}$, where the ULDM particle mass ratio $m_{21} = m/(10^{-21}{\rm eV}/c^2)$. This is slightly larger than the default value $\Delta t_d = 1.039\,m_{21}^{-1}{\rm yr}$ (of PyUltraLight2) [25], so we have tested the convergence and stability of our choice independently. For the further discussions on the similar choices of time resolution, see [26] and also [10, 27].

In our simulation below, we set the ULDM particle mass as $m = 10^{-21}{\rm eV}/c^2$ ($m_{21} = 1$) and place a central ULDM halo of mass $M_s = 10^9\,{\rm M}_\odot$ (hence $M = M_s$) at the center of the box to represent a galactic DM core. To clearly see the orbital decay, we choose a rather dense core. This central halo will be modeled by the ground state (soliton) configuration of the Schrödinger-Poisson system in the absence of BHs or any other particles. We then place two BHs of the same mass $M_{\rm bh}$ at $(\pm 0.45\,{\rm pc},\ 0,\ 0)$ respectively. To demonstrate the effect of the gravitational cooling, we generate 91 samples with uniformly varying $M_{\rm bh}$ from $0.6\times10^8{\rm M}_\odot$ to $1.5\times10^8{\rm M}_\odot$. In each sample, the initial velocity of each BH is chosen such that the corresponding initial orbit becomes nearly circular and the total simulation time set to be $T_{\rm total} = 100\,m_{21}^{-1}\,{\rm kyr}$.

III. NUMERICAL RESULTS

Figure 1 shows three snapshots of ULDM profiles with $M_{\rm bh} = 0.6\times10^8{\rm M}_\odot$; The initial profile is depicted on the left panel, the $t = 50\,{\rm kyr}$ on the middle, and the $t = 100\,{\rm kyr}$ on the right. As the two BHs are revolving around each other, their movement stirs the surrounding ULDM halos and generates ULDM waves. The central region of the ULDM profile becomes elliptical, indicating a dipole-like perturbation by the SMBHB. Part of these waves escape the central region while carrying away the kinetic energy of the BHB, which is nothing but the gravitational cooling effect. The time evolution of the binary separation $D(t)$ is our main concern here and depicted on the left panel of Figure 2 for $M_{\rm bh} = (0.7,\ 1.1,\ 1.4)\times10^8\,{\rm M}_\odot$. Note that our initial ULDM halo configuration is not stationary since the extra interaction, due to the BHB, was initially not taken into account. The presence of BHB subsequently makes

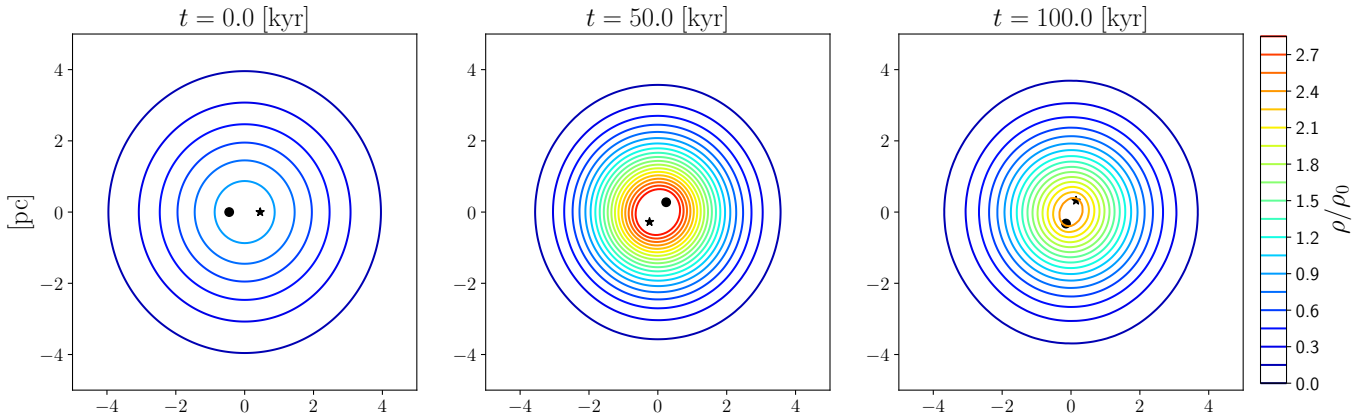

FIG. 1: Time evolution of the SMBHB of mass $M_{\rm bh} = 0.6 \times 10^8 {\rm M}_\odot$ inside ULDM halo of mass $M_s = 10^9 {\rm M}_\odot$. Colored lines represent the contour lines of ULDM density, where $\rho_0 = 7.05 \times 10^6\,(m_{21})^6\,{\rm M}_\odot/{\rm pc}^3$ denotes the initial central density of an isolated ground-state ULDM halo system. The black dot and star in each diagram stand for our BHB embedded. See Figure 2 for the orbital decay patterns. The BHs are revolving about 30 times within several periods of central density oscillations, whose details are not fully shown in this figure.

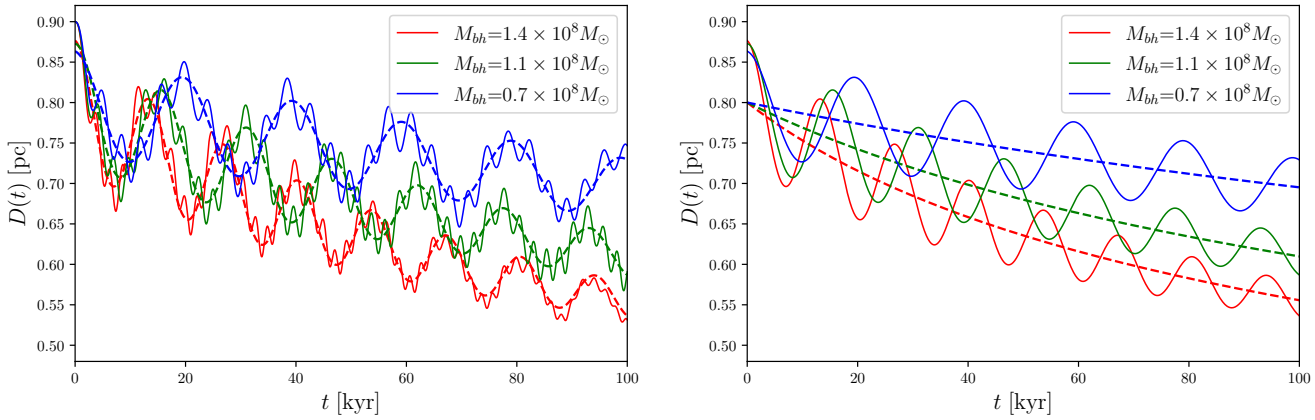

FIG. 2: Time evolution of BHB separation $D(t)$ for $M_{\rm bh} = (0.7, 1.1, 1.4) \times 10^8 {\rm M}_\odot$ (blue, green, and red lines). Left: simulated $D(t)$ (solid) and its full fit (dotted). Right: full fit of $D(t)$ (solid) and the *averaged* fit $\bar{D}(t)$ (dotted). See the texts for the definitions of full fit and averaged fit.

some ULDM halos attracted toward the BHs, and drives the ULDM halo system to oscillate radially together with the oscillation of the central ULDM density. This will be the major deriving force behind yet another gravitational cooling of the entire system.

As time progresses, the initial collapse will be quickly settled down with regular oscillations. The time evolution of $D(t)$ in general exhibits the slow and fast oscillations with a slowly decaying average $\bar{D}(t)$. Firstly, the fast oscillation is simply due to the slight eccentricity of the orbit and will be ignored in the following analysis. Next, the slow oscillation mainly follows from the global quasi-normal-mode [28] breathing of halo system together with the spherical central density oscillation, which is closely related to the gravitational cooling of the overall system. If there is no central BH, the time scale of this oscillation is of order of $\hbar^3/(m^3 G^2 M_s^2)$, where M_s is the mass of the soliton. In our case, SMBHB can slightly change the time scale ($T_{\rm slow}$ below). On the other hand, the decaying average $\bar{D}(t)$ seems to be related to another quasi-normal mode with a time scale τ_g from the local dipole perturbation by the rotating SMBHB at the center rather than by the global oscillation of the soliton. This mode is non-spherical and can carry away the angular momentum of the SMBHB (see Sec. IV for details).

In the remainder of this section, we shall focus on extracting the *averaged* orbital decay function $\bar{D}(t)$ largely independent of the slow global oscillations. However, there is no well-defined procedure for such averaging since the

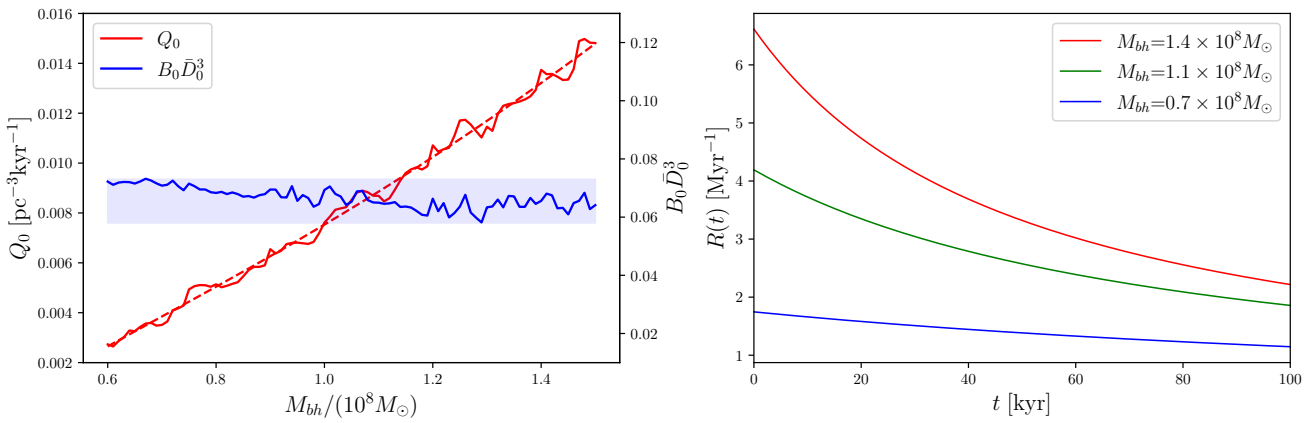

FIG. 3: Left: fitting parameters Q_0 (red line) and $B_0\bar{D}_0^3$ (blue line) as a function of $M_{\rm bh}$ derived from the simulations for $M_{\rm bh} = 0.6 - 1.5 \times 10^8 {\rm M}_\odot$. Red dotted line: the best-fit of $Q_0(M_{\rm bh})$ from the theoretical model described in Sec. IV. Light-blue shaded region emphasizes that $B_0\bar{D}_0^3$ is nearly constant over $M_{\rm bh}$. Right: time evolution of the decay rate of BHB separation $R(t)$ for $M_{\rm bh} = (0.7, 1.1, 1.4) \times 10^8 {\rm M}_\odot$ (blue, green, and red lines).

oscillations in Figure 2 are in their nonlinear regime. Ignoring the fast oscillation, we try the following fit function

$$D(t) = \bar{D}(t) + A_s\, e^{-\alpha_s t} \cos(\omega t - \phi)\,, \tag{4}$$

where the *averaged* function $\bar{D}(t)$ is defined by

$$\bar{D}(t) = \bar{D}_0 \left(1 + 3Q_0\, \bar{D}_0^3\, (t - t_0)\right)^{-1/3} \tag{5}$$

with the initial time $t_0 = 0$ in our case (see the next section for the derivation of (5)). We perform the $D(t)$ fitting with the fitting parameters, $(Q_0, \bar{D}_0,\, A_s, \alpha_s,\, \omega,\, \phi)$. For each of $M_{\rm bh} = (0.7,\, 1.1,\, 1.4) \times 10^8\, {\rm M}_\odot$, we depict the fit function of $D(t)$ as a dotted curve on the left panel and as a solid curve on the right panel of Figure 2. We have also added $\bar{D}(t)$ as a dotted curve for the comparison on the right panel. One finds $\bar{D}_0 \simeq 0.8\,{\rm pc}$ there. The Q_0 as a function of $M_{\rm bh}$ is depicted on the left panel of Figure 3. Using the parameters and the fit function $\bar{D}(t)$, one can also obtain the decay rate given by

$$R(t) \equiv -\frac{{\rm d}\log \bar{D}}{{\rm d}t} = \frac{Q_0 \bar{D}_0^3}{1 + 3Q_0 \bar{D}_0^3\, (t - t_0)}\,, \tag{6}$$

which is plotted on the right panel of Figure 3 for $M_{\rm bh} = (0.7,\, 1.1,\, 1.4) \times 10^8\, {\rm M}_\odot$.

In the above fit, we also obtain the slow oscillation period $T_{\rm slow} \equiv 2\pi/\omega$, which may be further fit with the formula

$$T_{\rm slow} = \frac{q_0 \hbar^3}{m^3 G^2 (M_s + 2\gamma_s M_{\rm bh})^2}\,, \tag{7}$$

where q_0 and γ_s are the fitting parameters. We numerically find that $q_0 \approx 86.28$ and $\gamma_s \approx 1.974$. Without the BHB, this time scale is well known (see for instance [27]). Here the main difference comes from the additional BH mass contribution weighted by the γ_s factor. In principle, the system may involve multiple quasi-normal modes which are characterised by the parameters $(q_0,\, \gamma_s)$. Especially, the quasi-normal mode caused by the orbital motion of BHB may involve different parameters as discussed in the next section.

Similarly to (4), the relative velocity of one BH with respect to the other can be fitted with the fit function given by

$$v_{\rm rel}(t) = \bar{v}_{\rm rel}(t) + \tilde{A}_s\, e^{-\tilde{\alpha}_s t} \cos(\tilde{\omega} t - \tilde{\phi}) \tag{8}$$

with $\bar{v}_{\rm rel}(t) = 2\sqrt{M_{\rm bh}(1 + B_0 \bar{D}^3)/(2\bar{D})}$, which is the twice of the rotation velocity of each BH including the ULDM contribution parameterized by $M_{\rm bh} B_0 \bar{D}^3 = 4\Delta M_s$ (see the next section for the details). The fitting parameter $B_0\bar{D}_0^3$ can be used for the consistency of our approximation in the next section and is depicted on the left panel of Figure 3.

IV. THEORETICAL ANALYSIS

In this section, we provide a rough estimate of the orbital decay timescale due to the gravitational cooling of the ULDM halo perturbed by a rotating SMBHB. This estimate is mainly based on dimensional analysis and intended to provide guidance for more accurate future calculations, because the system is highly nonlinear. Our simulation in the previous section suggests that the orbital decay is caused by the local gravitational cooling of the quasi-normal mode of the ULDM halo excited by the rotation of the BHs at the center.

Based on the scaling relations of the Schrödinger-Poisson equations, one may estimate momentum change of the BHB due to the quasi-normal mode radiation as follows. As was mentioned already, the ULDM waves generated by the BHB carry away the momentum and orbital energy of the BHs. The corresponding gravitational cooling timescale of the quasi-normal mode with SMBHB is given by $\tau_g = \hbar^3/(m^3 G^2 \tilde{M}_s^2)$ [28], where $\tilde{M}_s = M_s + 2\gamma M_{\rm bh}$ is an effective core mass determining the frequency of the quasi-normal mode from the ULDM halo mass combined with the BHB mass weighted by a factor γ. Since the perturbation has a local origin, this factor γ is in general slightly different from the global one (γ_s) in $T_{\rm slow}$ and will be determined separately below. Each BH is dragging some extra amount of ULDM distribution whose mass contribution is denoted by ΔM. The average gravitational force between the core halo and the induced ULDM mass ΔM is roughly given by $\bar{F}_g = G\tilde{M}_s \Delta M/r_h^2$, where the half-mass radius of the ULDM halo is $r_h = f_0 \hbar^2/(m^2 G \tilde{M}_s)$ with $f_0 = 3.925$ (see for instance [23]). Note also the magnitude of the momentum change of the ULDM halo should be balanced with that of the BHs. One may define the interacting time $\Delta\tau_c \equiv \pi \bar{D}/v$, which is approximately the orbital period of the BHs.

Collecting all these terms, the momentum change of each BH during one rotational period is roughly

$$\Delta p \equiv M_{\rm bh} \Delta v = K_0 \left(\frac{\Delta\tau_c}{\tau_g}\right) \left(\frac{G\tilde{M}_s \Delta M}{r_h^2}\right) \Delta\tau_c, \tag{9}$$

where K_0 is a numerical constant, and $\Delta\tau_c/\tau_g$ represents the cooling fraction of the effective impulse $\bar{F}_g \Delta\tau_c$ due to the gravitational cooling by the dipole perturbation. Dividing the both sides of (9) by $vM_{\rm bh}$ and using τ_g and r_h in the above, one may find the fractional velocity variation

$$\frac{\Delta v}{v} = K_0 \left(\frac{\pi \bar{D}}{r_h}\right)^2 \left(\frac{\hbar f_0}{m v r_h}\right)^3 \left(\frac{\Delta M}{M_{\rm bh}}\right). \tag{10}$$

Now we assume that the induced mass ΔM is proportional to the BH mass as $\Delta M = \alpha M_{\rm bh}(\pi\bar{D}/r_h)$, where $\alpha(M_{\rm bh}/M_s)$ is a dimensionless $\mathcal{O}(1)$ factor, and the ratio $\pi\bar{D}/r_h$ represents the fact that the BHB gives a dipole perturbation to the ULDM mass distribution proportional to the separation $\bar{D}$. Thus, the fractional velocity variation roughly becomes

$$\frac{\Delta v}{v} = \alpha\, K_0 \left(\frac{\pi \hbar f_0}{m v r_h^2}\right)^3 \bar{D}^3. \tag{11}$$

Assuming a circular orbit, the orbital velocity of BHs depends on both the BH mass ($M_{\rm bh}$) and the ULDM mass (ΔM_s) enclosed within the orbit, with Kepler's law: $v = \sqrt{G\tilde{M}_{\rm bh}/2\bar{D}}$ where $\tilde{M}_{\rm bh} \equiv M_{\rm bh} + 4\Delta M_s$. The central density is approximately $\rho_c \propto M_s/r_h^3$, and the enclosed mass within $\bar{D}/2$ is $\Delta M_s = 4\pi\rho_c(\bar{D}/2)^3/3 = \eta\, m_{21}^6 M_s \tilde{M}_s^3 \bar{D}^3 = (B_0 \bar{D}^3) M_{\rm bh}/4$, where η is a constant and B_0 is introduced in the previous section.

From now on, we assume $B_0 \bar{D}^3 \ll 1$ so that its contribution in $\tilde{M}_{\rm bh}$ is ignored in the computation below. We also checked that our simulations in Sec. III indeed satisfy this condition. Then, $v \propto \bar{D}^{-1/2}$ and $\left|\Delta\bar{D}/\bar{D}\right| = 2\left|\Delta v/v\right|$. By inserting the above expressions of v and r_h into (11), one can obtain

$$\left|\frac{\Delta\bar{D}}{\bar{D}}\right| = 2\alpha K_0 \left(\frac{2 f_0}{\pi}\right)^{\frac{3}{2}} \left(\frac{\pi\bar{D}}{r_h}\right)^{\frac{9}{2}} \left(\frac{\tilde{M}_s}{\tilde{M}_{\rm bh}}\right)^{\frac{3}{2}}. \tag{12}$$

Multiplying it with $1/\Delta\tau_c = v/(\pi\bar{D})$ gives an approximate differential equation for $\bar{D}(t)$,

$$-\frac{{\rm d}\log\bar{D}}{{\rm d}t} = \frac{4\pi^2 \alpha K_0 G^5 m^9 \tilde{M}_s^6}{{f_0}^3 \hbar^9 M_{\rm bh}} \bar{D}^3 = Q_0 \bar{D}^3, \tag{13}$$

where $Q_0 \equiv \kappa m_{21}^9 \tilde{M}_s^6/M_{\rm bh}$ with $\kappa = 4\pi^2 \alpha K_0 G^5 m^9/({f_0}^3 \hbar^9 m_{21}^9)$. This equation is perfectly consistent with the two scaling relations of our Schrödinger-Poisson system and may be integrated leading to (5).

m $[10^{-21}\mathrm{eV}/c^2]$	$M_{\rm bh}$ $[10^8\mathrm{M}_\odot]$	$T_{\rm total}$ [Gyr]	D_* [pc]
1	1	0.9926	0.03478
	10^{-1}	11.29	0.01136
5	1	2.524×10^{-4}	4.392×10^{-3}
	10^{-3}	8.503×10^{-2}	1.058×10^{-4}
	10^{-5}	2.284	7.618×10^{-6}

TABLE I: Examples of the total decay time ($T_{\rm total}$) and the corresponding separation scale (D_*) with various conditions of ULDM particle mass (m) and BH mass ($M_{\rm bh}$) when the ULDM halo mass is $M_s = 10^9\,\mathrm{M}_\odot$. Note that the decay happens within a Hubble time for most of SMBH mergers for $m = 5\times10^{-21}\mathrm{eV}/c^2$.

Based on the above analysis, we fit Q_0 in Figure 3 by assuming the quadratic form $\kappa = \kappa_0\left[1+10\,\delta_1(M_{\rm bh}/M_s)+100\,\delta_2(M_{\rm bh}/M_s)^2\right]$ with fitting parameters $(\gamma,\kappa_0,\delta_1,\delta_2)$. This fit of Q_0 is depicted on the left panel of Figure 3 by a dotted curve. One finds $\gamma\approx1.476$, $\kappa_0\approx2.958\times10^{-49}\,\mathrm{kyr}^{-1}\mathrm{pc}^{-3}\mathrm{M}_\odot^{-5}$ with negligibly small δ_1 and δ_2. These values for κ and Q_0 are used to estimate $T_{\rm total}$ below.

We now turn to a brief discussion of the requirement $B_0\bar{D}^3 \ll 1$ that is necessary for the consistency of the evolution equation (13). First of all, one may confirm that $B_0\bar{D}^3 \ll 1$ for our simulation since $B_0\bar{D}_0^3 \in [0.058, 0.073]$ (see Figure 3). For smaller value of $M_{\rm bh}$, one could have $B_0\bar{D}^3 \geq 1$ violating the requirement. But, in this case, the orbital decay rate ($\sim Q_0\bar{D}^3$) is generically expected to be enhanced even though the above approximation scheme breaks down. As $\bar{D}$ is decreasing further, there exists a moment t_* at which $B_0\,\bar{D}(t_*)^3 \ll 1$. From then, our evolution equation (13) becomes valid. Since the decay time from $\bar{D}_0$ to $\bar{D}(t_*)$ may in general take a relatively short time scale compared to the full decay time and may be safely ignored in the estimation of the full decay time.

As the separation $\bar{D}$ is decreasing further and further, the decay rate due to the ULDM halo becomes smaller and smaller while the rate due to the gravitational wave radiation becomes comparable to that of the ULDM halo. The separation scale at this moment will be denoted by D_*. If $\bar{D} < D_*$, the decay down to the horizon scale is mainly due to the gravitational wave radiation whose time scale is estimated as $T_{\rm gr}(D_*) = 5\,c^5D_*^4/(512\,G^3M_{\rm bh}^3)$ [29]. On the other hand, the decay time due to ULDM halo from $\bar{D}_0$ to D_* may be approximated by $T_{\rm dm}(D_*) = 1/(3Q_0D_*^3)$ assuming $D_*^3/\bar{D}_0^3 \ll 1$. To satisfy the condition $B_0\bar{D}_0^3 \ll 1$, we choose $\bar{D}_0 = (m_{\rm bh}/m_s)^{\frac{1}{3}}/(\tilde{m}_s m_{21}^2)\,\mathrm{pc}$ as an initial condition, where $m_{\rm bh} \equiv M_{\rm bh}/(10^8\mathrm{M}_\odot)$, $m_s \equiv M_s/(10^9\mathrm{M}_\odot)$, $\tilde{m}_s \equiv m_s + 0.2\gamma m_{\rm bh}$, and we set $\delta_1 = \delta_2 = 0$ for simplicity. However, as mentioned earlier, simply fixing the initial separation by $\mathcal{O}(\mathrm{pc})$ does not considerably alter our estimation. Minimizing the total decay time $T_{\rm total} = T_{\rm dm}(D_*) + T_{\rm gr}(D_*)$ with respect to D_*, one finds

$$T_{\rm total} = 2.409\,(m_{\rm bh}^5\tilde{m}_s^{24}m_{21}^{36})^{-\frac{1}{7}}\ \mathrm{Gyr} \tag{14}$$

with $D_* = 0.04342\left(m_{\rm bh}^4/(\tilde{m}_s^6m_{21}^9)\right)^{\frac{1}{7}}$ pc. Table I shows some explicit numbers with $m_s = 1$ ($M_s = 10^9\mathrm{M}_\odot$). Our analysis favors m_{21} somewhat larger than the fiducial value $m_{21} \simeq 0.1$.

V. SUMMARY

In this letter, we demonstrate through numerical simulations that ULDM waves generated by rotating BHBs in ULDM halos can cause rapid orbital decay and give a hint to the final parsec problem. This phenomenon was unexpected because the orbital decay of BHBs in ULDM halos is generally considered to be slow due to the weak dynamical friction [30]. The rapid decay of the orbits reported in this letter arises from the gravitational cooling of the halos perturbed by BHBs at galactic centers, which is a unique feature of ULDM. Another advantage of ULDM is that it is free from the loss cone problem, unlike CDM or collisionless stars. This is because ULDM has a wavelike nature, which helps it rapidly refill the phase space. Figure 1 shows that the central density of ULDM may even increase as the separation of the black holes decreases unlike CDM.

These findings have implications for future gravitational wave probes like LISA or NANOGrav, as ULDM waves can change the orbital properties of the SMBHBs and influence gravitational waves generated by them, especially when their separation is small. To further validate our results, higher-resolution simulations are planned for future studies.

Acknowledgments

This research was supported by Basic Science Research Program through the National Research Foundation of Korea (NRF) funded by the Ministry of Education (2018R1A6A1A06024977) for HK, DB and IP. DB was also supported in part by NRF Grant RS-2023-00208011. SEH was supported by the project "Understanding Dark Universe Using Large Scale Structure of the Universe" funded by the Ministry of Science. This work was supported by the Korea Institute of Science and Technology Information, through the KREONET network and the supercomputing resources.

[1] M. C. Begelman, R. D. Blandford, and M. J. Rees, Nature **287** (1980) 307.
[2] Milosavljević, Miloš, and David Merritt, AIP Conference Proceedings. Vol. 686. No. 1. (2003).
[3] G. Agazie *et al.* [NANOGrav], Astrophys. J. Lett. **952** (2023) no.2, L37.
[4] M. R. Baldeschi, G. B. Gelmini and R. Ruffini, Phys. Lett. B **122** (1983) 221.
[5] M. Membrado, A. F. Pacheco and J. Sañudo,Phys. Rev. A **39** (1989) 4207.
[6] S.-J. Sin, Phys. Rev. **D50** (1994) 3650.
[7] J.-W. Lee and I.-G. Koh, Phys. Rev. **D53** (1996) 2236.
[8] F. S. Guzman and T. Matos, Class. Quant. Grav. **17** (2000) L9.
[9] W. Hu, R. Barkana and A. Gruzinov, Phys. Rev. Lett. **85** (2000) 1158.
[10] S. Park, D. Bak, J. W. Lee and I. Park, JCAP **12** (2022) 033.
[11] W. J. G. de Blok, A. Bosma and S. S. McGaugh, astro-ph/0212102 (2002).
[12] A. Tasitsiomi, International Journal of Modern Physics D **12** (2003) 1157.
[13] T. Matos and D. Nunez, Rev. Mex. A.A. 44 (2008) 149.
[14] J. P. Mbelek, Astron. Astrophys. **424** (2004) 761–764.
[15] T. H. Lee and B. J. Lee, Phys. Rev. D **69** (2004) 127502.
[16] H.-Y. Schive, T. Chiueh and T. Broadhurst, Nature Physics **10** (2014) 496–499.
[17] T. H. Lee and B. J. Lee, Phys. Rev. Lett. **123** (2019) 021102.
[18] D. J. E. Marsh, Phys. Rept. **643** (2016) 1.
[19] J.-W. Lee, Journal of Korean Physical Society **54** (2009) 2622.
[20] A. Suárez, V. H. Robles, and T. Matos, Astrophysics and Space Science Proceedings **38** (2014) 107.
[21] T. Rindler-Daller and P. R. Shapiro, Modern Physics Letters A **29** (2014) 1430002.
[22] P.-H. Chavanis, Phys. Rev. D **84** (2011) 043531.
[23] L. Hui, J. P. Ostriker, S. Tremaine, and E. Witten Phys. Rev. D **95** (2017) 043531.
[24] Seidel, E., and Suen, W. M. Phys. Rev. D 42(2) (1990) 384.
[25] Y. Wang, R. Easther, arXiv:2110.03428.
[26] F. Edwards, E. Kendall, S. Hotchkiss and R. Easther, JCAP **10**, (2018) 027.
[27] D. Bak, J.-W. Lee and S. Park, J. Korean Phys. Soc. **79**, no.6, (2021) 582.
[28] F. Siddhartha Guzmán and L. Arturo Ureña-López, Phys. Rev. D 69 (2004) 124033.
[29] Peters, P., Phys. Rev. **136** (1964) 1224.
[30] R. Vicente and V. Cardoso Phys. Rev. D **105** (2022) 083008.